

## Clay mineral authigenesis in coal and shale from the Anthracite region, Pennsylvania

ERIC J. DANIELS, STEPHEN P. ALTANER

Department of Geology, University of Illinois, 1301 W. Green St., Urbana, Illinois 61801, U.S.A.

### ABSTRACT

Textural, chemical, and mineralogical analyses of authigenic clays in anthracite-rank coal and associated shale from eastern Pennsylvania have allowed a better understanding of the parameters controlling diagenesis and perhaps coalification in this region. Minerals in anthracite occur in distinct assemblages associated with the following microenvironments: coal matrix, two orthogonal joint sets (termed systematic and nonsystematic cleat), and a third joint set. Mineralogical differences among microenvironments allow inferences about clay-mineral origins and the parameters that controlled mineral authigenesis. Kaolinite occurs in the shale, and all microenvironments within the coal seam. Authigenic minerals that replaced preexisting kaolinite during the latest stage of coalification (anthracitization) at  $T > 200$  °C include  $\text{NH}_4$ -rich illite, pyrophyllite, and the following minerals, which are primarily restricted to the systematic cleat set: tosudite (R1-ordered, dioctahedral, mixed-layer chlorite/smectite), sudoite (di, trioctahedral chlorite) and rectorite (R1-ordered, mixed-layer paragonite/smectite). Alteration of smectite to illite may be responsible for formation of authigenic illite and Na-bearing illite, which are present only in the shale and coal matrix, and Fe-, Al-rich chlorite and quartz in the third joint set. The chemical components for authigenesis appear to have multiple sources: Al and Si from preexisting kaolinite and quartz, N from local organic matter, Mg and Na (for tosudite, sudoite, and rectorite) largely from metasomatic hydrothermal fluids, Fe and Mg for Fe-, Al-rich chlorite from smectite illitization.

Minerals in the shale, the coal matrix, and the nonsystematic cleat set are interpreted to represent authigenesis in a low-permeability environment (closed-system alteration); however, the assemblage sudoite + tosudite + rectorite in the systematic cleat set is interpreted to be the result of one or two stages of hydrothermal alteration (open-system alteration). We suggest that differences in minerals between the two nearly perpendicular cleat sets are the result of permeability differences which were maintained by an anisotropic lateral stress field created by plate convergence during the Alleghanian orogeny. Hydrothermal alteration may be related to large-scale basinal flow induced by Alleghanian-age uplift; such migrating fluids could also have transported heat from depth and thereby significantly increased the rate and rank of coalification in this region.

### INTRODUCTION

Coal maturation is a function of the diagenetic history of a region and it is, therefore, important to understand all processes that may affect coalification. Authigenic clay minerals are often used as geothermometers (Hoffman and Hower, 1979) and as indicators of the geochemistry of diagenetic fluids in sedimentary rocks and, thus, are invaluable tools for oil, gas, and ore exploration. Mineral assemblages can also be used to infer modes of diagenesis (e.g., hydrothermal alteration vs. burial diagenesis), to indicate compositions of diagenetic fluids, and to reconstruct the diagenetic history of a region. For example, Tillman and Barnes (1983) used fluid inclusions and textural relationships among minerals in joint sets in Paleozoic rocks from northern New York to determine the paragenetic sequence of authigenesis and jointing, as well as fluid compositions and temperatures during authigenesis.

In this study, we examine the distribution, texture, structure, and composition of authigenic clay minerals in anthracite and associated shale from eastern Pennsylvania to determine mineral origins. The data give insight into the influence of tectonics on diagenesis of inorganic and perhaps organic phases. The results also allow a more complete interpretation of the origins of the minerals in the adjacent shale, which are ambiguous because the shale contains a multicomponent assemblage of intimately intergrown detrital and authigenic minerals.

### Geology and mineralogy of the Anthracite region, Pennsylvania

The Anthracite region of eastern Pennsylvania is the oldest coal mining district in the United States and constitutes one of the largest anthracite deposits in the world. The Pennsylvanian Llewellyn and Pottsville Formations, which contain over 40 minable coal seams, outcrop in

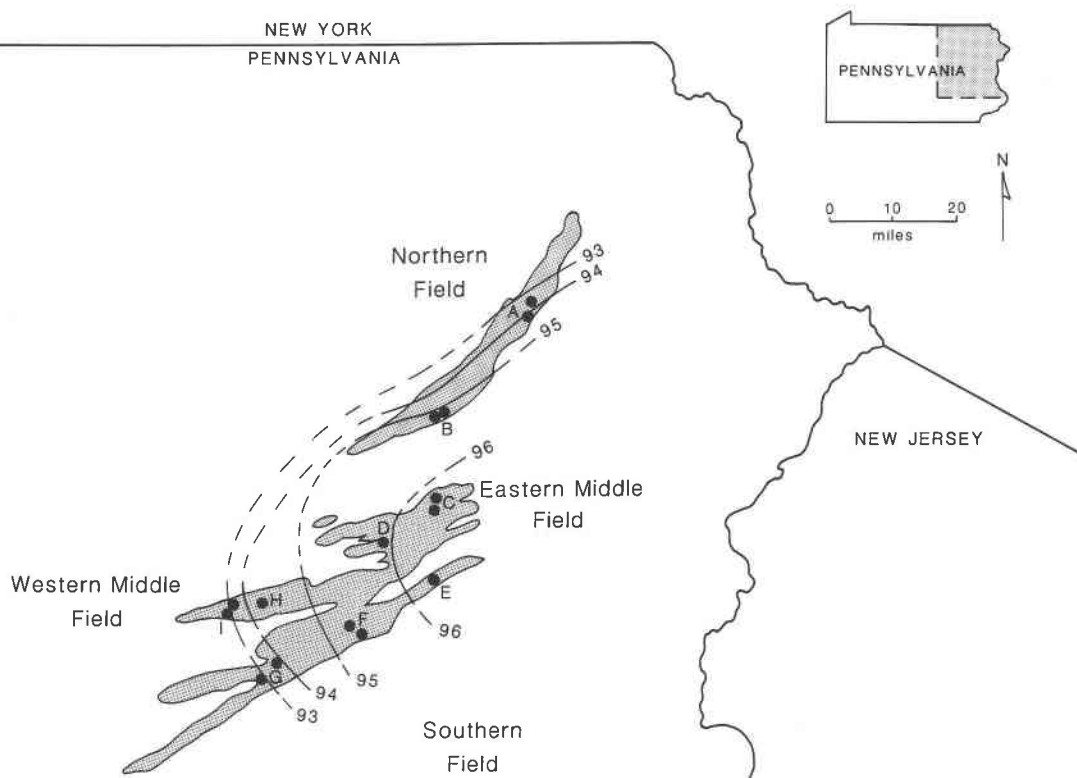


Fig. 1. Map of the Anthracite region of eastern Pennsylvania. Fixed C isograds and sample localities are also shown. Letters A-I correspond to sample localities used in tables and text. (Modified from Deasy and Greiss, 1961.)

four coal fields in the easternmost part of the Valley and Ridge Province in Pennsylvania (Fig. 1; Wood et al., 1969).

Most mineralogical studies of sediments in this region have been concerned with shale (underclay) adjacent to the coal seams. An early study by Schultz (1958) showed that underclay in this region contains illite, kaolinite, quartz, and chlorite. In addition to these clays, Hosterman et al. (1970) identified pyrophyllite and suggested that it formed at the expense of kaolinite and quartz during peak metamorphism. Recently, Paxton (1983) and Juster et al. (1987) showed that some of the illite-like minerals in these richly organic shales contain large amounts of  $\text{NH}_4^+$  substituting for  $\text{K}^+$  in the illite interlayer. Paxton (1983) suggested that the N source was dispersed organic matter in the shale and that  $\text{NH}_4$ -rich illite formed from kaolinite, whereas Juster et al. (1987) concluded that N was derived from adjacent coal seams and that  $\text{NH}_4$ -rich illite formed from illite by substitution of  $\text{NH}_4^+$  for  $\text{K}^+$ . All studies indicate that the concentrations of authigenic minerals (pyrophyllite, chlorite, and  $\text{NH}_4$ -rich illite) in the shales increase (along with coal rank) to the south and east and that no highly expandable (smectitic) clays are present.

Most of the published mineralogical studies of anthracite categorize minerals into general structural types (e.g.,

swelling and nonswelling clays, carbonates, sulfides, etc.) for the purpose of assessing the effects of these minerals on the mining, preparation, and uses of the coal. Although minerals in coal can occur in the dense organic matrix and in joints, most mineralogical analyses have been carried out on combusted (ashed) whole-coal samples, thus precluding separate analysis of mineral assemblages in the matrix and joints. In the only published detailed mineralogical study of coal from the Anthracite region, Spackman and Moses (1961) determined that minerals in the coal are similar to those found in associated shale. They also showed that mineralogic variations occur both within and between coal seams and that chlorite and pyrophyllite contents increase with the degree of deformation.

Systematic joints (commonly termed cleat) are often found in coal seams, yet their origin and significance are poorly understood. Cleat are thought to form by dewatering and volume reduction of the organic matter caused by compression during the early stages of coal diagenesis or in response to regional stresses after lithification (Stach, 1975). In Pennsylvania, bituminous coal and anthracite usually contain a joint system composed of two nearly orthogonal sets of well-formed cleat that are approximately perpendicular to bedding ( $90^\circ \pm 10^\circ$ ). The strike of the systematic cleat set ( $J_3$ ) is roughly perpendicular to

the local trend of the Alleghanian orogenic belt and the nonsystematic cleat set ( $J_{NS}$ ) strikes nearly perpendicular to  $J_S$  (Nickelsen and Hough, 1967). Nickelsen (1979) concluded that this cleat system probably formed prior to or during the earliest stages of Alleghanian deformation. Another joint set found in Pennsylvania coal seams, which will be referred to as  $J_3$ , formed in both the coal and adjacent shale during a later, more intense deformational stage of the Alleghanian orogeny (Nickelsen, 1979). In the rocks of the present study, the strike of  $J_S$  is generally northwest, that of  $J_{NS}$  northeast and that of  $J_3$  north-northeast (Daniels et al., 1990).

Cleat minerals in bituminous- and lower-rank coal deposits have been the subject of numerous studies. Kaolinite and quartz are the only silicates observed in cleat in Pennsylvania (Nickelsen and Hough, 1967), Illinois (Hatch et al., 1976), England (Spears and Caswell, 1986), and Canada (Van der Flier-Keller and Fyfe, 1988). These silicates probably precipitated during early diagenesis (Spears and Caswell, 1986). Presumably, Al and Si migrate (in a gel or colloidal form) out of the organic matter, and eventually recrystallize in cleat as kaolinite and quartz. Al and Si are initially concentrated in a peat swamp owing to intense cation leaching of detrital minerals caused by acidic conditions and the action of plants which selectively absorb alkali elements for nutrition and which may secrete silica (Mackowsky, 1975). Other minerals observed in coal cleat include carbonates and sulfides in the Illinois Basin (Hatch et al., 1976) and zeolites in the Colorado Plateau (Finkelman et al., 1987).

## METHODS

Fifteen coal and forty shale samples were collected from five outcrops and ten strip mine exposures of the Llewellyn Formation throughout the Anthracite region. All shale samples were rich in organic material and located near coal seams. An approximate measure of the rank of coal and associated shale samples were determined by plotting sample localities on a base map containing previously determined fixed carbon (FC) values for coal seams throughout the area (Deasy and Greiss, 1961; Fig. 1). FC values (calculated on a dry ash-free basis) in coal increase linearly with rank and, thus, maximum diagenetic temperature (Teichmüller and Teichmüller, 1975). Correlations by Levine (1983) of vitrinite reflectance data with the level of organic maturation (LOM) scale of Hood et al. (1975) suggest that maximum diagenetic temperatures in the Anthracite region varied across the region from 210–260 °C,  $\pm 15$  °C. Some coal and shale samples that were taken from scrap piles in the Northern Fields were not assigned FC values because the original locations of these samples could not be determined.

Coal samples required special preparation before analysis because they contain minerals disseminated throughout the organic matrix and in various joints. Flakes of clay in the joints of coal samples were separated from the organic matrix with a razor blade, hand-ground, dispersed by sonification, and then analyzed by X-ray dif-

fraction (XRD). Numerous flakes from each sample were gently scraped away from the organic matrix to observe textural relationships among the minerals by scanning electron microscopy (SEM). When both  $J_S$  and  $J_{NS}$  were present in a single sample, flakes from each cleat set were carefully collected separately for mineral identification by XRD, SEM, and transmitted-light optical petrography. After all the flakes were removed, the remaining coal matrix was ground in a ball mill and sieved to less than 74  $\mu\text{m}$ . The organic material was combusted following a low-temperature ashing procedure, which concentrates mineral matter without significantly altering the composition or structure of silicates (Gluskoter, 1965), and the resultant ash was analyzed by XRD.

Scanning electron microscopy (SEM), using a JEOL JSM 840A scanning electron microscope equipped with a Kevex 7500 energy dispersive X-ray (EDX) analyzer and a back-scattered electron detector, was used primarily to determine the distribution, qualitative chemical analyses, concentration, and morphology of minerals in the coal joints. Mineral flakes were also examined with an optical petrographic microscope. Many flakes in this study are relatively flat and have thicknesses of  $\sim 30$ – $50$   $\mu\text{m}$  and, hence, were simply placed on glass slides for examination. A combination of SEM/EDX analysis and optical petrography can be used to clearly distinguish between the clay minerals, based on their physical and compositional characteristics.

XRD data were obtained using a Siemens D500 diffractometer, equipped with  $\text{CuK}\alpha$  radiation. Randomly oriented powder mounts were studied in order to determine clay mineral polytypes and whole rock mineral assemblages. All samples of size fractions  $< 2$   $\mu\text{m}$  were X-rayed in the air-dried and glycolated states and scanned from both  $2$ – $32$   $^{\circ}2\theta$  and  $43$ – $48$   $^{\circ}2\theta$  at a scanning speed of  $1^{\circ}$  per min and with a time constant of 1 s.

X-ray diffraction was used to determine semiquantitative estimates of mineral concentrations in whole samples and size fractions  $< 2$   $\mu\text{m}$  of most samples (Table 1 and Fig. 7). Characterization and quantification of clay minerals were aided by the calculation of  $00l$  XRD intensities, using the computer program Newmod (written R. C. Reynolds, Dartmouth College, New Hampshire). Estimates of mineral concentrations for samples with significantly different mineral assemblages probably have errors of approximately  $\pm 30$  wt%. However for samples with similar mineral assemblages, errors are estimated to be  $\pm 10$  wt% (Bayliss, 1986). Mineral concentrations in  $J_S$  and  $J_{NS}$  (Table 1) are of the size fraction  $< 2$   $\mu\text{m}$  and, thus, quantities of coarse-grained minerals such as quartz may have been underestimated.

Cell parameters and  $hkl$  indices for  $\text{NH}_4$ -rich illite (Table 2) were calculated with a least-squares cell-refinement program (Appleman and Evans, 1973). The concentration of  $\text{NH}_4$  (mol%) in  $\text{NH}_4$ -rich illite was estimated by using the 005 XRD reflection (Fig. 2), where mol%  $\text{NH}_4$  is the percent of interlayer sites occupied by  $\text{NH}_4$ . It was used to calculate  $d(001)$ , with the assumption of a linear

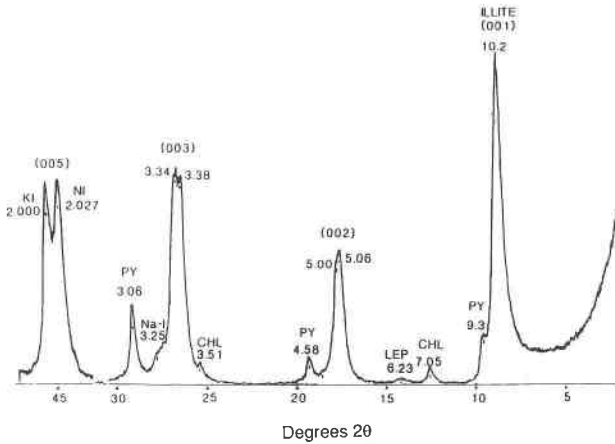


Fig. 2. X-ray diffraction pattern of shale from locality D (<2 μm, oriented, air-dried) showing increased resolution of 00l reflections of illite and NH<sub>4</sub>-rich illite at higher 2θ positions. NI = NH<sub>4</sub>-rich illite, KI = illite, CHL = Fe-rich chlorite; LEP = lepidocrocite, Na-I = Na-bearing illite ("brammallite"), PY = pyrophyllite. 2–30°2θ region was scanned at twice the vertical range value used in the 43–47°2θ region. D values are in Å.

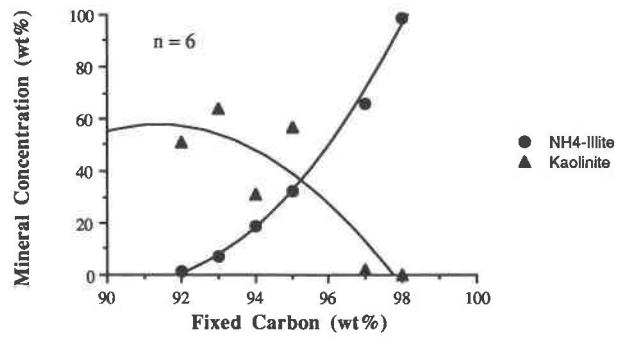


Fig. 3. Concentration of NH<sub>4</sub>-rich illite (circles) and kaolinite (triangles) in coal matrices vs. fixed C.

relation between d(001) of illite (10 Å; Bailey, 1980) and end-member NH<sub>4</sub>-rich illite (10.35 Å; Eugster and Munoz, 1966). For example, by this method, the NH<sub>4</sub>-rich illite for which XRD data are given in Figure 2 (d<sub>005</sub> = 2.027 Å) contains 39 mol% NH<sub>4</sub> and 61 mol% K. Inorganic N (i.e., N residing in illite) concentrations were calculated by the following formula:

$$\text{wt\% N} = X_{\text{NH}_4} \times 4.78 \times X_{\text{NI}} \times 0.79$$

TABLE 1. Coal mineralogy of the size fraction <2 μm

Sample	Local-ity*	Micro**	Kaolin-ite	Quartz	Illite	NH <sub>4</sub> -rich illite	Fe-Al-rich chlorite	Pyro-phyllite	Tosu-dite	Sudoite	Rec-torite	Others
1	D	Matrix	77†	—	17	—	—	—	—	—	—	Na-bearing illite (6)
		J <sub>s</sub>	12	3	—	—	—	3	23	45	14	—
		J <sub>NS</sub>	5	23	—	—	—	59	7	6	—	—
2	E	Matrix	2	21	<1	66	3	—	—	—	—	Na-bearing illite (8)
		J <sub>s</sub>	23	—	—	21	—	—	1	55	—	—
		J <sub>NS</sub>	32	—	—	48	—	—	3	17	—	—
3	E	Matrix	—	—	—	62	5	—	—	—	—	Paragonite (8); siderite (10)
		J <sub>s</sub>	2	13	—	—	85	—	—	—	—	Diaspore (7); boehmite (8)
		J <sub>NS</sub>	37	—	—	55	8	—	—	—	—	Na-bearing illite (9)
4	F	Matrix	4	—	30	49	8	—	—	—	—	Na-bearing illite (9)
		J <sub>s</sub>	7	—	—	10	83	—	—	—	—	—
		J <sub>NS</sub>	37	—	—	55	8	—	—	—	—	—
5	F	Matrix	52	—	33	—	—	—	—	—	—	Na-bearing illite (7); goethite (8)
		J <sub>s</sub>	21	—	—	—	51	3	—	—	25	—
		J <sub>NS</sub>	50	—	—	—	12	—	—	—	38	—
6	H	Matrix	97	—	2	—	—	—	—	—	—	Boehmite (1)
		J <sub>s</sub>	52	—	—	—	—	34	14	—	—	—
		J <sub>NS</sub>	92	—	—	—	—	6	2	—	—	—
7	H	Matrix	31	37	9	19	1	—	—	—	—	Na-bearing illite (3)
		J <sub>s</sub>	54	—	—	30	—	—	16	—	—	—
		J <sub>NS</sub>	1	—	—	99	—	—	—	—	—	—
8	C	Matrix	—	—	—	99	<1	—	—	—	—	Rutile (<1)
		J <sub>s</sub>	<1	—	—	3	<1	—	—	—	95	Pyrite (1); barite (<1)
9	A	Matrix	57	—	33	7	<1	—	—	—	—	Na-bearing illite (3)
		J <sub>s</sub>	59	—	—	—	—	—	41	—	—	—
10	A	J <sub>s</sub>	21	—	—	—	76	3	—	—	—	—
		J <sub>NS</sub>	62	—	—	—	1	—	—	—	—	Na-bearing illite (2)
11	B	Matrix	45	—	52	—	—	—	—	—	—	—
		J <sub>s</sub>	62	—	—	—	—	30	5	—	3	—
12	F	J <sub>s</sub>	5	51	—	—	23	18	3	—	—	—
		J <sub>NS</sub>	57	—	9	32	1	—	—	—	—	Lepidocrocite (1)
13	F	Matrix	57	<1	—	—	<1	34	6	—	—	—
		J <sub>s</sub>	59	<1	—	—	<1	34	6	—	—	—
14	G	Matrix	64	5	23	7	—	—	—	—	—	Na-bearing illite (<1); lepidocrocite (1)
		J <sub>s</sub>	51	28	15	1	2	—	—	—	—	Rutile (3)

\* Localities are shown in Figure 1.

\*\* Micro = mineralized microenvironments observed in each sample.

† Numbers represent mineral concentration in weight percent.

where  $X_{\text{NH}_4}$  = mole-fraction  $\text{NH}_4$  substitution in  $\text{NH}_4$ -rich illite, 4.78 = wt%  $\text{NH}_4$  in  $\text{NH}_4$  end-member muscovite,  $X_{\text{NI}}$  = weight fraction of  $\text{NH}_4$ -rich illite in the sample based on XRD data, and 0.79 = weight fraction of N in  $\text{NH}_4$ . XRD estimates of N contents in whole-rock samples are consistent with total N analyses (Daniels, 1989).

Microprobe analyses were obtained using a JEOL 50-AX Microprobe equipped with a Tracor-Northern EDX analyzer (beam diameter = 2  $\mu\text{m}$ ). Analyses were carried out using polished thin sections of mineral flakes from coal fractures or polished sections of shale chips. Prior to analyses, samples were embedded in epoxy, polished with a diamond lap and then carbon coated. Monomineralogical flakes from coal fractures were used whenever available to provide the most accurate chemical composition for a particular mineral. Such analyses include those for  $\text{NH}_4$ -rich illite, sudoite, rectorite, and pyrophyllite. Because N cannot be detected with the EDX detector, the XRD-based estimate of  $X_{\text{NH}_4}$  was used to calculate wt%  $\text{NH}_4$  in the  $\text{NH}_4$ -rich illite structural formula. The chemical analyses for tosudite, muscovite, and illite were obtained from samples that contained other minerals, according to XRD. However, SEM examination revealed that these minerals occur in book- or nestlike aggregates of monomineralogical crystallites >40  $\mu\text{m}$  in diameter and, hence, such chemical analyses were probably not affected by contamination by other phases.

## RESULTS

### Coal mineral assemblages

The mineral assemblages of the coal in the Anthracite region are extremely interesting and complex because minerals in the coal often differ from those in the associated shale and because the coal itself can contain at least four assemblages (Table 1). One assemblage occurs in the dense organic matrix of the coal. The other assemblages are found in the three joint sets ( $J_s$ ,  $J_{\text{NS}}$ , and  $J_3$ ) that permeate many coal samples.

The coal matrix contains 4–25 wt% inorganic material. Minerals observed in the coal matrix are similar to those observed in the coal by Spackman and Moses (1961) and in the associated shale units by Paxton (1983) and Juster et al. (1987), except that the coal matrix contains no pyrophyllite. The major minerals are illite ( $2M_1$  polytype),  $\text{NH}_4$ -rich illite ( $1M$  polytype), kaolinite, and quartz. Minor minerals include Fe-rich chlorite, Na-bearing illite ("brammallite"), rutile, lepidocrocite, goethite, and boehmite. Some of the highest-rank coals (e.g., in locality E) contain paragonite, diaspore, and siderite (Table 1). Kaolinite is the most prevalent mineral in most coal matrices, with  $\leq 96\%$  FC, yet makes up <2 wt% of the matrix minerals in higher-rank anthracites.  $\text{NH}_4$ -rich illite is present in nearly every anthracite-rank coal sample, and its concentration in the coal matrix increases with increasing coal rank (Fig. 3). The other minerals in the coal matrix show no significant trends with respect to coal rank.

**TABLE 2.** X-ray diffraction data for  $\text{NH}_4$ -bearing illite (with 70 mol%  $\text{NH}_4$  substitution) in the coal matrix from locality C

<i>hkl</i>	$d_{\text{obs}}$	$l/l_0$	<i>hkl</i>	$d_{\text{obs}}$	$l/l_0$
001	10.3	100	132	2.222	8
002	5.13	42	133	2.170	12
020	4.49	100	005	2.049	12
111*	4.36	55	231	1.968	8
021*	4.12	21	232	1.919	4
112*	3.69	72	224	1.845	5
003	3.41	58	135	1.691	19
112*	3.10	55	060,244	1.503	31
113*	2.97	9			
023*	2.718	17			
131	2.570	75			
104	2.492	8			
131	2.451	17			
132	2.409	20			
201	2.370	9			
040,033	2.250	9			

$a = 5.225 \text{ \AA}$   
 $b = 8.996 \text{ \AA}$   
 $c = 10.447 \text{ \AA}$   
 $\beta = 101.47^\circ$

\* Indicates reflections that are diagnostic of  $1M$  mica polytype.

The cleat sets are filled with thin, translucent flakes that contain many minerals, including  $\text{NH}_4$ -rich illite, kaolinite, tosudite, rectorite, pyrophyllite, sudoite, quartz, and trace amounts of pyrite, barite, gypsum, and another S-bearing phase (native S?). Kaolinite and quartz persist throughout the region in both cleat and other joint sets. Although present in the coal matrix, authigenic illite, Na-bearing illite, and rutile are not present in any of the coal joints. Cleat flakes commonly contain large detrital grains of organic material, and one sample from locality B contains cleat flakes with minor amounts of large anhedral (presumably detrital) grains of partially altered muscovite. Detrital particles were probably severed from the joint face during joint formation and subsequently entrapped in a matrix of authigenic minerals.

Monomineralic flakes of  $\text{NH}_4$ -rich illite occur in coal matrices and cleat from all four Anthracite fields, where it occurs in dense packets of straight and curved crystallites 10  $\mu\text{m}$  to 50  $\mu\text{m}$  in length (Fig. 4A). In all samples,  $\text{NH}_4$ -rich illite occurs as a  $1M$  polytype, indicated by XRD reflections at 4.36  $\text{\AA}$ , 4.12  $\text{\AA}$ , 3.69  $\text{\AA}$ , 3.10  $\text{\AA}$ , 2.97  $\text{\AA}$ , and 2.718  $\text{\AA}$  (Table 2). All of these reflections have larger  $d$  values than corresponding  $hkl$  reflections for  $1M$  illite (Bailey, 1980) owing to the presence of interlayer  $\text{NH}_4$ , which causes an increase in the magnitude of the  $c$  axis.  $\text{NH}_4$ -rich illite may contain up to 5% expandable layers, as shown by changes in positions, widths, and intensities of peaks following ethylene glycol treatment (Fig. 5). Microprobe analyses (Table 3) show that  $\text{NH}_4$ -rich illite has an Al-Si ratio nearly equal to 1, a dioctahedral structure (2.0 octahedral cations/ $\text{O}_{10}(\text{OH})_2$ ) and a trace amount of Fe.

The amount of  $\text{NH}_4$  in  $\text{NH}_4$ -rich illite from both the cleat and matrix of most coal samples is similar (67–76 mol%) although it is considerably less in the lower-rank anthracite samples (20–30 mol%). The amount of  $\text{NH}_4$  substitution in  $\text{NH}_4$ -rich illite from shale varies considerably and does not appear to be related to coal rank (Fig.

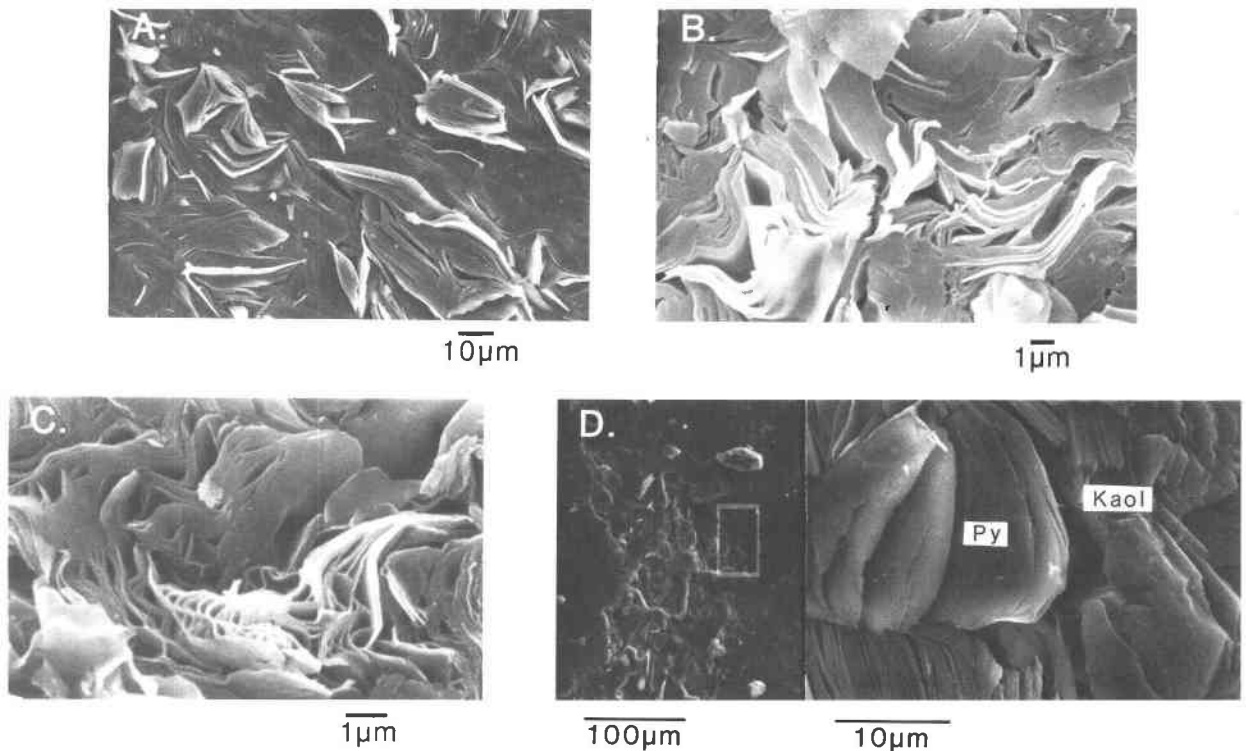


Fig. 4. SEM photomicrographs of minerals in cleat sets. (A) Large, elongate  $\text{NH}_4$ -rich illite in  $J_{NS}$  from locality G. (B) Small, wavy tosudite in  $J_S$  from locality B. (C) Wavy rectorite in  $J_S$  from locality C. (D) Pyrophyllite in a large dissolution pit on a kaolinite-dominated flake in  $J_S$  from locality H.

6). These observations differ from those of Juster et al. (1987), who observed a decrease in  $\text{NH}_4$  substitution in  $\text{NH}_4$ -rich illite (from shale samples) with increasing coal rank and suggested that this reflected a miscibility gap between K-rich and  $\text{NH}_4$ -rich illite at  $T < 400^\circ\text{C}$ .

Pyrophyllite is abundant in the joints of five coal samples, where it is intimately associated with (i.e., found on the same flakes as) kaolinite, quartz, and tosudite. Interestingly, pyrophyllite is absent in all of the coal matrices (even though the adjacent shale beds and coal cleat may be relatively pyrophyllite-rich) and pyrophyllite occurs only in those coal joints that contain no  $\text{NH}_4$ -rich illite (Table 1). This observation is best illustrated by comparing the matrix and cleat mineral assemblages of sample 13, and by comparing the clear mineral assemblages of samples 6 and 7, which were both obtained from the same coal seam at locality H, but approximately 300 m apart.

Expandable, ordered mixed-layer clay minerals have not been previously reported as occurring in this region, yet they are present in nearly every  $J_S$  set examined. Tosudite (aluminous, dioctahedral, mixed-layer chlorite/smectite with 50% chlorite layers and regular alternation of layers, or R1-order) occurs in relatively significant quantities (5–40 wt% of  $< 2\ \mu\text{m}$  size fraction) in  $J_S$  from six coal samples and in minor amounts ( $< 5$  wt% of  $< 2\ \mu\text{m}$  size fraction) in  $J_{NS}$  and  $J_3$  in some of those samples.

Identification of tosudite by XRD is based on rational basal reflections corresponding to a superlattice spacing of  $28\ \text{\AA}$  in an air-dry state that expands to  $31\ \text{\AA}$  upon glycolation (Fig. 5). Flakes containing tosudite are brown or tan in plane-polarized light. It occurs in wavy packets of crystallites approximately  $5\ \mu\text{m}$  long (Fig. 4B) and as pseudomorphs after kaolinite. At a relatively lower coal rank, it is associated with (i.e., found on the same flakes as) kaolinite and minor amounts of quartz, whereas at higher coal ranks it also occurs with sudoite and pyrophyllite. Microprobe analysis indicates that it has an Al-Si ratio nearly equal to 1, octahedral occupancy = 3.31 atoms/ $\text{O}_{10}(\text{OH})_5$ , and contains small amounts of Mg and Fe (Table 3). The anion content is  $\text{O}_{10}(\text{OH})_5$  because this mineral contains 50% smectite ( $\text{O}_{10}(\text{OH})_2$ ) and 50% chlorite ( $\text{O}_{10}(\text{OH})_8$ ). For an  $\text{O}_{10}(\text{OH})_5$  formula unit, 3 octahedral cations would represent a pure dioctahedral composition and 4.5 octahedral cations would represent a pure trioctahedral composition. The aluminous and nearly dioctahedral composition of chlorite/smectite in the Anthracite region distinguishes it from corrensite (a trioctahedral, Mg-rich chlorite/smectite with R1-order and 50% chlorite layers), which has identical 00/ spacings and can have similar relative intensities of the basal reflections.

Rectorite (R1-ordered, mixed-layer Na-rich mica/smectite with 50% Na-rich mica layers) is present in  $J_S$

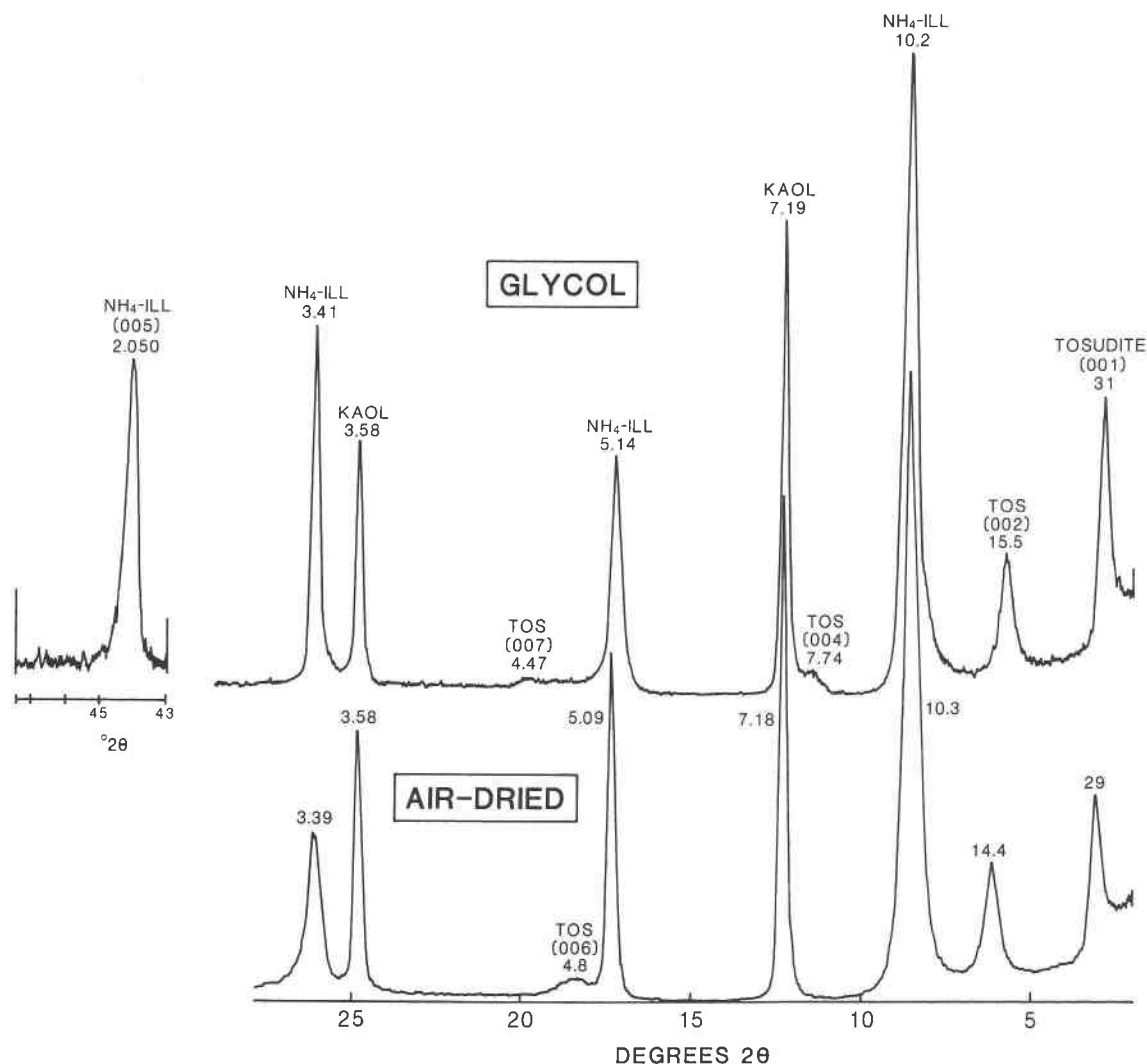


Fig. 5. X-ray diffraction pattern of minerals in both joint sets of a coal sample from locality H. The relative increase of the  $\text{NH}_4$ -rich illite (003) peak height and small shift in the (002) d-value after saturation with ethylene glycol indicates that this phase contains ~5% smectite layers. KAOL = kaolinite, TOS = tosudite. The 2–30  $2\theta$  region was scanned at twice the vertical range used in the 43–47  $2\theta$  region.

from four localities and in  $J_{NS}$  in one of those samples. No other clay minerals occur in those flakes that contain rectorite. In coal from locality C, it makes up 95 wt% of the size fraction  $<2 \mu\text{m}$  of the joint mineral assemblage and is intimately associated with pyrite, barite, gypsum, and an S-bearing phase (native S?). Identification of rectorite by XRD is based on rational basal reflections corresponding to a superlattice of 24 Å in the air-dry state that increases to 27 Å upon glycolation. Rectorite exhibits both a cornflake-like morphology and a morphology similar to that of tosudite and  $\text{NH}_4$ -rich illite (Fig. 4C). Microprobe analyses of rectorite reveal a high Na and a low K content (Table 3).

Two types of chlorite are observed in joints from the Anthracite region. One chlorite is a trioctahedral, Fe- and Al-rich variety that makes up 23–85 wt% of the  $<2 \mu\text{m}$

minerals in  $J_3$  from three localities and is associated with quartz, pyrophyllite, and kaolinite. Fe- and Al-rich chlorite also occurs in the cleat of two samples; it usually is massive and anhedral. In samples 10 and 12 (Table 1), chlorite appears to have precipitated as a coating over a mat of anhedral quartz, whereas in sample 3 it is intergrown with anhedral quartz grains. Microprobe analyses yield octahedral occupancies ranging from 5.7 to 5.85 cations per  $\text{O}_{10}(\text{OH})_8$ , suggesting either that the hydroxide sheets are not fully trioctahedral or that the analysis is contaminated by quartz.

The second type of chlorite, sudoite (chlorite with one aluminous dioctahedral sheet and one Mg-rich trioctahedral sheet), is associated with tosudite in  $J_s$  from two samples of the highest rank coals in the Southern and Eastern Middle Fields ( $\text{FC} \geq 97\%$ ). Minor amounts of

TABLE 3. Chemical analyses and structural formulae of phyllosilicates from eastern Pennsylvania

	Rectorite [C]	NH <sub>4</sub> - rich illite [H]	Pyro- phyllite [B]	Mus- covite [C, shale]	Illite [F, shale]	Fe-, Al-rich chlorite		Sudoite		Tosudite	
						[A]	[E]	[E]	[D]	[F]	
SiO <sub>2</sub>	52.28	49.42	65.96	47.60	48.39	SiO <sub>2</sub>	19.20	24.40	34.74	33.17	41.21
Al <sub>2</sub> O <sub>3</sub>	35.32	38.13	33.34	33.04	27.19	Al <sub>2</sub> O <sub>3</sub>	24.38	23.17	36.69	33.71	35.88
Fe <sub>2</sub> O <sub>3</sub> *		0.50		3.13	2.54	FeO†	20.59	28.10	3.42	7.00	2.73
MgO				0.74	1.95	MgO	6.49	12.38	12.92	8.88	1.86
TiO <sub>2</sub>				0.43	0.58	MnO	0.33				
K <sub>2</sub> O	0.76	2.36		9.58	6.94	K <sub>2</sub> O					1.20
Na <sub>2</sub> O	4.83			1.36							
(NH <sub>4</sub> ) <sub>2</sub> O**		4.90									
Total wt% oxides†	93.19	95.31	99.30	95.88	87.60	Total wt% oxides†	71.00	88.04	87.77	82.76	82.89
		Cations/O <sub>10</sub> (OH) <sub>2</sub>					Cations/O <sub>10</sub> (OH) <sub>8</sub>				Cations/ O <sub>10</sub> (OH) <sub>5</sub>
Tetrahedral cations						Tetrahedral cations					
Si	3.33	3.12	3.80	3.15	3.41	Si	2.48	2.64	3.10	3.21	3.40
Al	0.67	0.88	0.20	0.85	0.59	Al	1.52	1.36	0.90	0.79	0.60
Octahedral cations						Octahedral cations					
Al	2.00	1.96	2.06	1.72	1.67	Al	2.18	1.60	2.96	3.05	2.89
Fe <sup>3+</sup>		0.03		0.16	0.13	Fe <sup>2+</sup>	2.21	2.29	0.25	0.52	0.19
Mg				0.07	0.21	Mg	1.26	2.00	1.73	1.28	0.23
Ti				0.02	0.03	Mn	0.04				
Σ <sub>oct</sub>	2.00	1.99	2.06	1.97	2.04	Σ <sub>oct</sub>	5.69	5.89	4.94	4.85	3.31
Interlayer cations						Interlayer cations					
K	0.07	0.19		0.81	0.62	K					0.12
Na	0.59			0.17							
NH <sub>4</sub>		0.71									

Note: Letters in brackets refer to localities in Figure 1. Samples are from flakes in coal joints unless noted otherwise.

\* Fe in the 2:1 clays was calculated as Fe<sub>2</sub>O<sub>3</sub>.

\*\* Wt% (NH<sub>4</sub>)<sub>2</sub>O was calculated from X-ray diffraction data.

† Oxide totals do not include structural water.

‡ Fe in the chlorite and tosudite was calculated as FeO.

sudoite are also observed in J<sub>NS</sub> in these samples. The 001/003 intensity ratio for sudoite (~0.1) is distinct from that of the Fe- and Al-rich chlorite (~1.0). The observed relative intensities of 00/*l* basal reflections for sudoite (*d*<sub>001</sub> = 14.15 Å) are 001 = 10, 002 = 80, 003 = 100, 004 = 55, and 005 = 10. Microprobe analyses show a range in octahedral occupancy from 4.85 to 5.05 cations per O<sub>10</sub>(OH)<sub>8</sub> (Table 3), suggesting that one octahedral sheet

is trioctahedral and the other is dioctahedral. A previous investigation of sudoite concluded that the Mg-rich trioctahedral sheet is the interlayer sheet (Lin and Bailey, 1985). Sudoite appears to have replaced tosudite and occurs in dense packets of wavy crystallites that are similar in size and morphology to some tosudite crystallites.

Although only J<sub>S</sub> cleat in some of the coal samples contain minerals, both J<sub>S</sub> and J<sub>NS</sub> cleat in other samples contain minerals. Detailed examination of six coal samples from localities D, E, F, and H show that mineral assemblages in J<sub>S</sub> are significantly different from those in J<sub>NS</sub> in all but one of the samples (Table 1). In five samples, J<sub>NS</sub> contains mostly NH<sub>4</sub>-rich illite and kaolinite or, in one case, pyrophyllite, kaolinite, and quartz, whereas J<sub>S</sub> contains kaolinite, tosudite, sudoite, pyrophyllite, Fe- and Al-rich chlorite, and rectorite in addition to NH<sub>4</sub>-rich illite. In the other sample, J<sub>S</sub> is enriched in Fe- and Al-rich chlorite, but rectorite is distributed equally between the two cleat sets.

There is some overlap in the lists of minerals in J<sub>S</sub> and J<sub>NS</sub>, as determined by XRD. Some of this overlap may be due to incomplete separation of the flakes from different joint sets during sample preparation. In addition, SEM and petrographic analyses show that flakes from J<sub>NS</sub> contain isolated veins of J<sub>S</sub>-type minerals, and that some J<sub>S</sub> flakes contain discrete zones of pure NH<sub>4</sub>-rich illite.

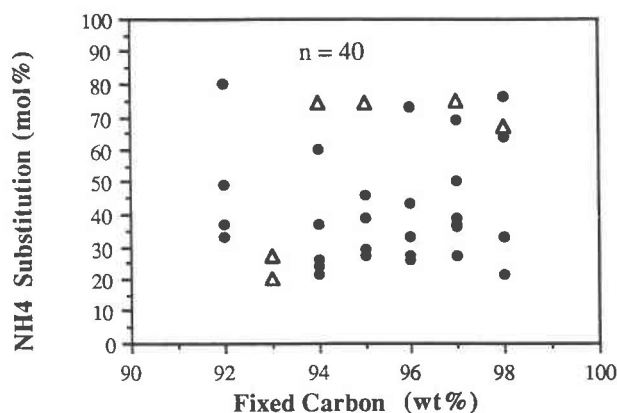


Fig. 6. Mol% NH<sub>4</sub> substitution in NH<sub>4</sub>-bearing illite from shale (circles) and coal (triangles) samples vs. fixed C.



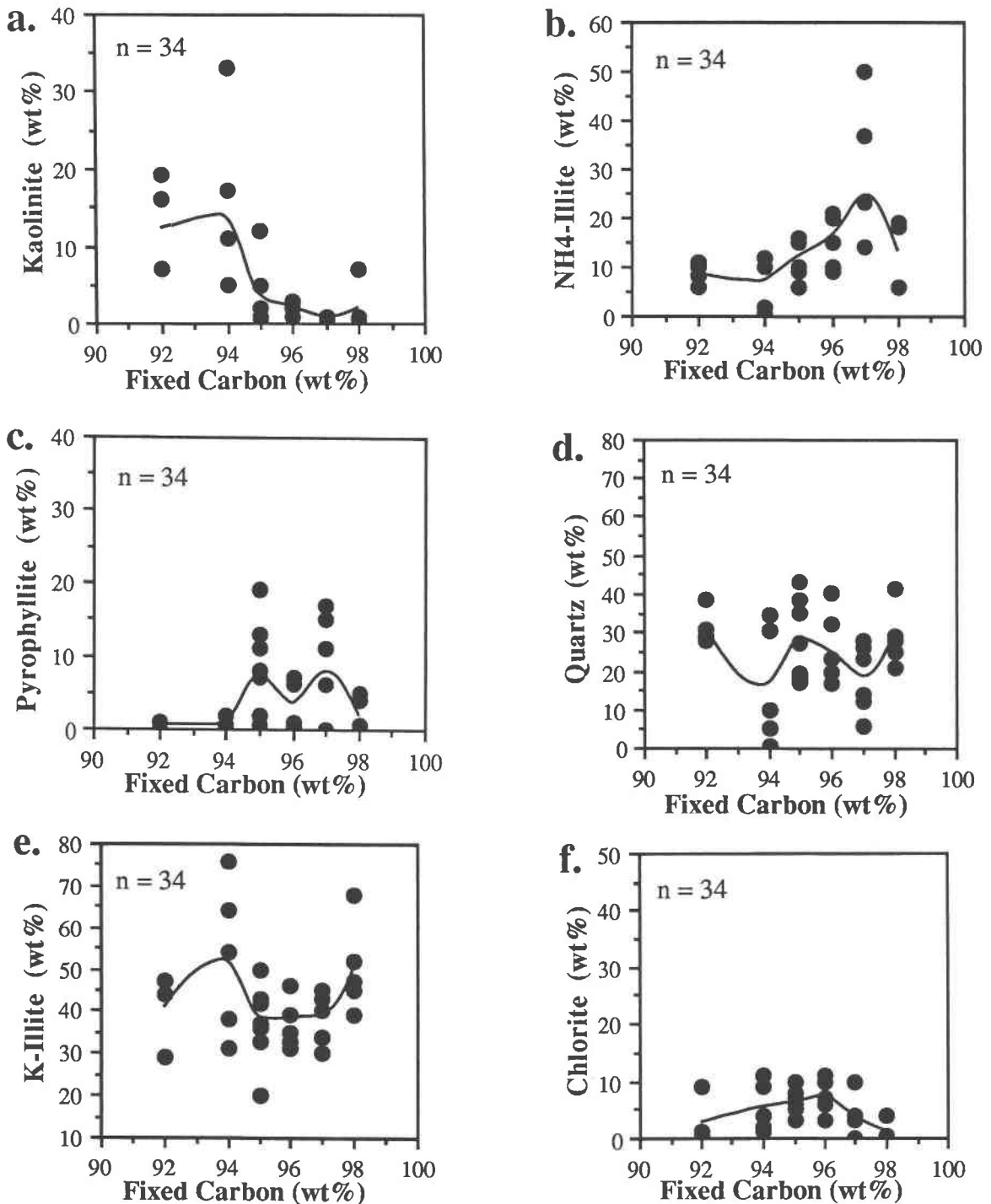


Fig. 7. Concentrations of kaolinite (a), NH<sub>4</sub>-rich illite (b), pyrophyllite (c), quartz (d), illite (e), and Fe-rich chlorite (f) in shale samples vs. fixed C. Lines represent average mineral concentrations.

#### Shale mineral assemblages

The shale minerals are discussed here only briefly because the results are similar to those of Paxton (1983)

and Juster et al. (1987). The dominant minerals observed are illite, NH<sub>4</sub>-rich illite, kaolinite, chlorite, pyrophyllite, and quartz. Minor or trace amounts of Na-bearing illite ("brammallite"), paragonite, pyrite, rutile, anatase, bar-

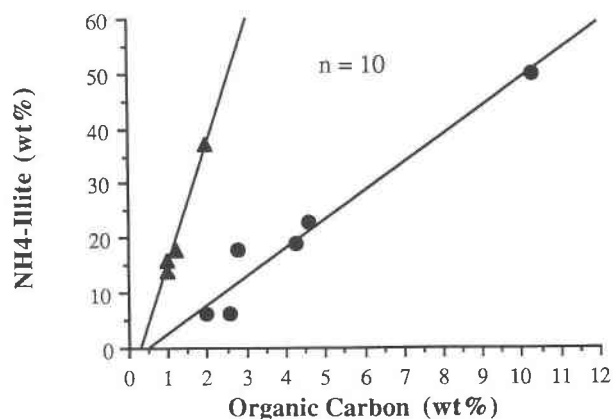


Fig. 8. Wt%  $\text{NH}_4$ -rich illite in shale of similar fixed-C content (FC = 97%) vs. the amount of organic matter in the samples. Triangles represent shale sampled directly underneath coal seams and circles represent shale sampled a farther, but unknown, distance away from coal seams.

ite, gypsum, cerrusite ( $\text{PbCO}_3$ ), lepidocrosite, and goethite occur in many samples. Shale from locality E contains numerous microfractures ( $J_3$ ) filled with Fe-rich chlorite; these samples also contain minor quantities of tosudite and R1-ordered, mixed-layer illite/smectite with ~70% illite layers.

Although there is considerable variation for a given FC value, the following general conclusions can be made about mineralogical variations in the shale as a function of coal rank. With increasing rank, kaolinite content decreases,  $\text{NH}_4$ -rich illite and pyrophyllite contents increase, and illite, quartz, and chlorite contents do not vary systematically (Fig. 7). Numerous factors complicate these trends, such as original mineralogical differences among samples and errors in estimates of FC values.

The amount of  $\text{NH}_4$ -rich illite in shale appears to increase with increasing amount of organic matter and with decreasing distance from the coal seams (Fig. 8). Shale from directly beneath coal seams (triangles in Fig. 8) has much greater values of the ratio of  $\text{NH}_4$ -rich illite to organic content than shale from an unknown, but most likely greater, distance from the coal seams (circles in Fig. 8).

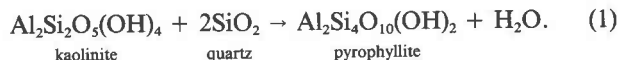
Microprobe analyses show that two types of illite coexist in some samples: fine-grained (presumably authigenic) illite with a net negative layer charge of ~-0.7, and coarse-grained illite with a muscovite-like composition that may be detrital and derived from a high-grade metamorphic environment (Table 3). No evidence was found for interstratified illite/ $\text{NH}_4$ -rich illite or paragonite/illite, both of which were described by Juster et al. (1987).

## DISCUSSION

### Clay mineral authigenesis in the Anthracite region

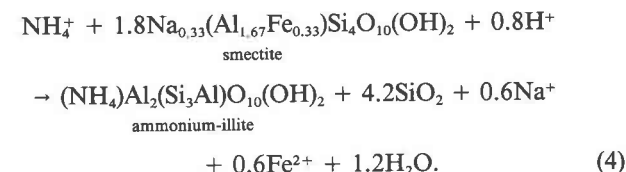
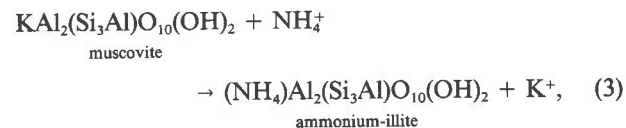
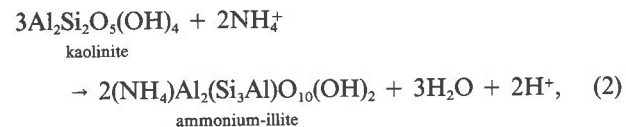
A number of interesting authigenic clay reactions have occurred during anthracitization. The most prominent reactions observed in the shale are the formation of py-

rophyllite and  $\text{NH}_4$ -rich illite. As suggested by Hosterman et al. (1970), pyrophyllite appears to have formed by the reaction



Hydrothermal experiments show that this reaction proceeds at  $T \geq 300^\circ\text{C}$  (Hemley et al., 1980). Pyrophyllite can form at lower temperatures, however, if  $a_{\text{H}_2\text{O}}$  is decreased, according to LeChatelier's principle. As suggested by Juster (1987), growth of authigenic pyrophyllite at 225–275  $^\circ\text{C}$  probably occurred in areas containing methane-rich fluids, where  $a_{\text{H}_2\text{O}}$  would be significantly less than 1.0. In most cases, pyrophyllite does not completely replace kaolinite, and it often occurs in apparent dissolution pits on kaolinite-dominated flakes (Fig. 4D). This incomplete reaction may be due to (1) disequilibrium, perhaps enhanced by the presence of immiscible methane-rich and water-rich fluids (Juster, 1987), (2) lack of available quartz, or (3) slow reaction rates. In locality B, anomalously small amounts of quartz in the coal and shale suggest that the quartz contents may have limited pyrophyllite formation. Samples 1 and 12 contain kaolinite, quartz, and pyrophyllite in proximity on the same flake, thereby supporting the argument for slow reaction rates.

$\text{NH}_4$ -rich illite can potentially form by at least three reactions:



Most of the data in this study, particularly mineral assemblages in the coal, support a kaolinite precursor. Kaolinite is ubiquitous in cleat from the Anthracite region, as well as in the semi-anthracite and bituminous fields west of this region. In addition, kaolinite is the only phyllosilicate observed in cleat from bituminous coal deposits in many other sedimentary basins (Hatch et al., 1976; Spears and Caswell, 1986; Van der Flier-Keller and Fyfe, 1988). In the Anthracite region, kaolinite contents decrease and  $\text{NH}_4$ -rich illite contents increase in both coal and shale as the rank increases (Figs. 3 and 7). Using a study of anthracite-rank shale in eastern Pennsylvania,

Juster et al. (1987) suggested that  $\text{NH}_4$ -rich illite formed by exchange of  $\text{NH}_4$  for K (reaction 3), because of intimate associations of illite and  $\text{NH}_4$ -rich illite as well as similar polytypes ( $2M_1$ ). In this study, pure  $\text{NH}_4$ -rich illite isolated from both coal matrix and cleat is observed to have a  $1M$  structure (Table 2), in contrast to a  $2M_1$  polytype observed for illite within both the coal matrix and the shale. XRD data indicate a  $1M$  polytype for  $\text{NH}_4$ -rich illite in the shale as well, although this was more difficult to determine definitively because of the presence of other minerals in the shale.

Authigenic  $\text{NH}_4$ -rich illite most likely formed at high temperatures associated with anthracitization and derived N from locally abundant organic matter. These conclusions are strongly supported by two observations: (1)  $\text{NH}_4$ -rich illite is observed only in coals of semi-anthracite or higher rank, and (2) significant amounts of organically bound N are lost from the coal as rank increases from bituminous coal to anthracite (Paxton, 1983).  $\text{NH}_4$ -rich illite must, therefore, have formed at temperatures corresponding to at least this coal rank ( $T \geq 200$  °C). The occurrence of  $\text{NH}_4$ -rich illite in  $J_{\text{NS}}$  is significant because it indicates that this joint set probably formed prior to anthracitization, in contrast with results of Nickelsen and Hough (1967), who concluded that  $J_{\text{NS}}$  in coal beds from the Alleghany Plateau probably formed as release-type joints when overburden was removed in post-Permian time.

Paxton (1983) concluded that the dispersed organic matter in the shale was the most likely N source, whereas Juster et al. (1987) concluded that the coal seams were the primary N source. Although both the dispersed organic matter in the shale and the larger amount of organic matter in nearby coal seams are potential N sources for  $\text{NH}_4$ -rich illite formation in the shale, the coal must have served as a major N source for certain shale samples, as shown by the following calculation. Organic matter in bituminous coal generally contains a maximum of 2.5 wt% N (Slatick, 1980). Thus, if a shale contains 10 wt% organic matter, it could provide a maximum of 0.25 wt% N for  $\text{NH}_4$ -rich illite formation, if one assumes complete transferral of N from organic matter to the silicate host. Most shales in this study contain  $\ll 10$  wt% organic matter (Fig. 8), yet some of these samples contain  $>0.25$  wt% inorganic N on a whole-rock basis (Fig. 9). Therefore, the coal, with a much greater concentration of organic matter, probably provided much of the N found in  $\text{NH}_4$ -rich illite in the adjacent shale. Data in Figure 8 suggest that for shale immediately adjacent to the coal seams, the coal contributed most of the N in  $\text{NH}_4$ -rich illite because the organic contents of these samples are low, yet their  $\text{NH}_4$ -rich illite contents are quite high. It is possible that, for shale farther from the coal seams, a larger percentage of the N in  $\text{NH}_4$ -rich illite was derived from dispersed organic matter in the shale.

Authigenic Fe- and Al-rich chlorite in coal and shale may have formed from kaolinite, by means of the reaction

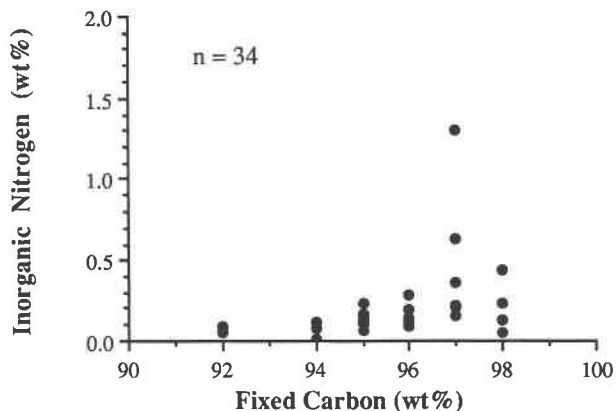
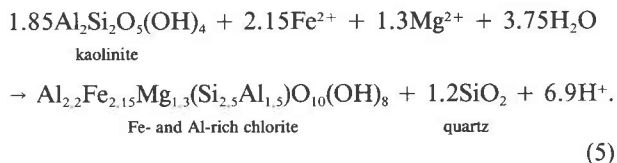
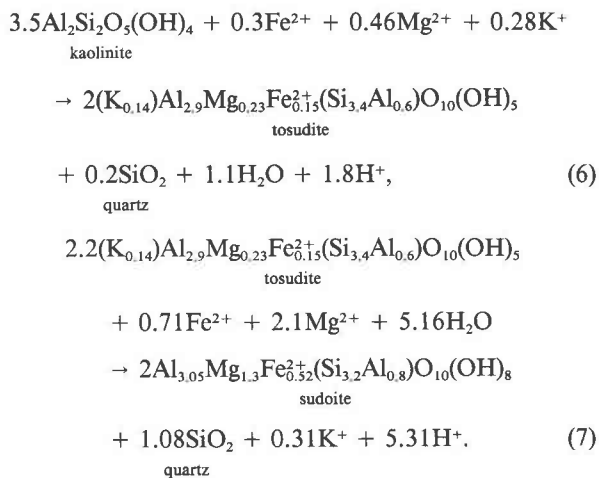


Fig. 9. Wt% inorganic nitrogen (N in  $\text{NH}_4$ -rich illite) in whole-shale samples vs. fixed-C content.



Fe, Mg and Si released during formation of illite from smectite may have promoted formation of authigenic Fe- and Al-rich chlorite and quartz. Authigenic chlorite that is compositionally similar to the Fe- and Al-rich chlorite of this study is observed in deeply buried Texas Gulf Coast sandstones, where  $T = 150$ – $200$  °C (Boles and Franks, 1979), and in bituminous-rank ( $130$ – $180$  °C) sandstones in north-central Pennsylvania (Paxton, 1983). In both the Texas Gulf Coast and north-central Pennsylvania, illite formation from illite/smectite is observed over approximately the same temperature range as formation of authigenic chlorite ( $100$ – $175$  °C and  $150$ – $180$  °C, respectively). Authigenic formation of Fe- and Al-rich chlorite and quartz in the  $J_3$  joint set also appears to have occurred during bituminization because the formation of joint set  $J_3$  postdates cleat formation and early diagenesis (Nickelsen, 1979), yet some of the kaolinite in the  $J_3$  joint set has been altered to pyrophyllite, suggesting that initial mineralization of joint set  $J_3$  occurred prior to anthracitization. In addition, small amounts of fine-grained tosudite have precipitated over the chlorite/quartz assemblage in one sample, suggesting that formation of authigenic chlorite occurred prior to tosudite formation. Formation of authigenic quartz may also have resulted from Si released from pressure solution of quartz grains in closely associated sandstones during diagenesis.

Another important series of reactions recorded in the Anthracite region is the formation of authigenic tosudite and sudoite in coal cleat. The following reactions are proposed for their formation:



Although previous studies of natural occurrences of tosudite (e.g., Shirozu, 1978; Morrison and Parry, 1986) and experimental studies (Eberl, 1978) indicate that tosudite can form from a smectite precursor, we observed direct evidence of a kaolinite precursor, but no evidence for a smectite precursor in cleat from any coal bed in Pennsylvania.

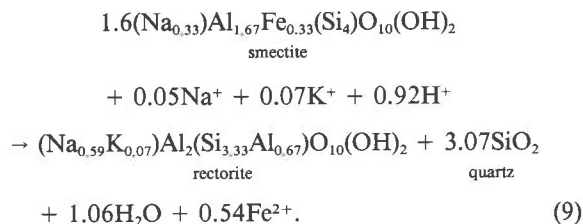
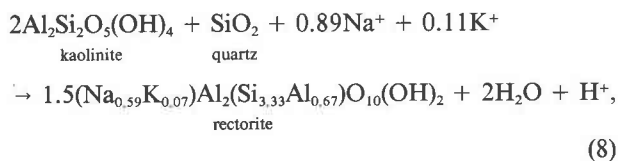
The intimate association of tosudite and sudoite in the higher-rank samples suggests that sudoite may form from tosudite, rather than from direct replacement of kaolinite. The formation of sudoite (di-, trioctahedral chlorite) from tosudite (dioctahedral chlorite/smectite) can be accomplished with precipitation of trioctahedral interlayers in place of the smectite interlayers of tosudite and with a change in the composition of the dioctahedral hydroxide interlayer sheet of tosudite. In addition, reaction 6 requires at least partial dissolution and reprecipitation of tetrahedral sheets (to increase the negative charge of the 2:1 layer) because the calculated ratio of Si to <sup>[4]</sup>Al in sudoite is significantly less than in tosudite (Table 3). However, it is impossible to determine the precise extent of recrystallization of the tetrahedral sheets because the compositions of the various tetrahedral and octahedral sheets in both minerals are unknown.

Although the temperatures at which these chlorite phases generally form in nature are not well constrained, they probably formed in these strata at  $T \geq 200$  °C because kaolinite is apparently unaltered in bituminous and semi-anthracite coal cleat and is altered to various degrees in anthracite cleat. Sudoite may have formed at higher temperatures (225–260 °C) than tosudite because sudoite occurs only in the highest-ranked samples in the Anthracite region. Fransolet and Schreyer (1984) concluded from hydrothermal experiments that sudoite is stable at approximately the same temperatures as pyrophyllite.

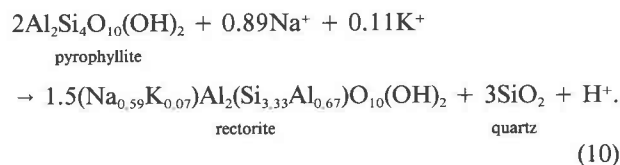
Formation of authigenic sudoite and tosudite in the cleat (which requires a source of Mg and Fe) probably was associated with fluids with a different composition than those fluids associated with alteration of smectite to illite and Fe- and Al-rich chlorite because sudoite and

tosudite are typically observed in hydrothermally altered Al-rich strata (Gradusov, 1971; Fransolet and Bourguignon, 1978; Shirozu, 1978), yet they are not observed in basins where transformation of smectite to illite is the dominant reaction, as in the Texas Gulf Coast. Chlorite that formed by means of the transition of smectite to illite typically has Fe/Mg ratios  $\geq 1.0$  (e.g., Boles and Franks, 1979), whereas the sudoite and tosudite observed in this study have Fe/Mg ratios  $< 1.0$ . In addition, illite/smectite is completely converted to illite at temperatures corresponding to low-volatile bituminous rank ( $\sim 180$  °C) in Pennsylvania (Paxton, 1983), whereas sudoite and tosudite appear to have formed at  $T \geq 200$  °C.

Na-rich rectorite may form from a kaolinite or smectite precursor:



Henderson (1971) has suggested that rectorite may form indirectly from kaolinite through pyrophyllite as an intermediate phase:



Rectorite observed in this study most likely formed directly from kaolinite. The formation of rectorite by reactions 9 and 10 is unlikely because both reactions produce relatively large amounts of quartz (which is not observed in the rectorite-dominated cleat) and because smectite is not observed in these or other cleat. Based on studies of natural occurrences of rectorite (e.g., Paradis et al., 1983) and its occurrence in only the highest-rank anthracites in this study, we suggest that rectorite probably formed at 225–260 °C.

The occurrence of tosudite, sudoite, and rectorite in the Anthracite region suggests that hydrothermal alteration influenced diagenesis in this area because those minerals are almost exclusively associated with hydrothermally altered Al-rich rocks and hydrothermal ore deposits in Al-rich terrains (tosudite: Shimoda, 1969; Gradusov, 1971; sudoite: Shirozu, 1978; Fransolet and Bourguignon, 1978; rectorite: Miser and Milton, 1964; Sudo and Shimoda,

1978; Nishiyama and Shimoda, 1981; Paradis et al., 1983). The fact that these clay minerals occur only in joints from the Anthracite region also suggests a hydrothermal origin. Although there are no known igneous intrusions that can account for hydrothermal alteration of this region during Pennsylvanian time, regional migration of basinal fluids in the Appalachian foreland basin, induced by Alleghanian-age orogenic uplift on the eastern flank of the basin, may have produced similar results. The extremely high coal rank in this region may also be a result of basinal fluid migrations, because fluids flushed out of deeper formations in the basin could have transported heat upward into the Pennsylvanian strata. In addition, enhanced heat flow into this region due to fluid migrations would (1) account for the relatively rapid coalification of organic matter in this region (postulated by Levine, 1986) and (2) result in a decrease in the postulated minimum burial depth (6–10 km) at which the coal attained anthracite rank in this area (Daniels et al., 1990).

Minerals restricted to the coal matrix may be detrital or authigenic phases. Rutile is common in many coal deposits and probably precipitated during peat accumulation. Deeply buried shales typically contain both detrital illite and authigenic illite formed from smectite (Hower et al., 1976). Microprobe analyses of a coarse-grained mica of probable detrital origin and fine-grained illitic minerals of probable diagenetic origin (Table 3) support the idea of mixed origins for illite. The occurrence of authigenic Na-bearing illite ("brammallite") and paragonite in the coal matrix and shale suggests that diagenetic fluids were K-poor. We interpret the absence of both illite and Na-bearing illites in the coal joints to indicate that these minerals probably formed from precursor phases other than kaolinite, possibly mixed-layer illite/smectite. The minor, yet ubiquitous Fe-rich chlorite in the coal matrix may be detrital, a product of alteration of smectite to illite, or both. Minor quantities of goethite, lepidocrocite, and boehmite are most likely the result of recent weathering.

### Mineral paragenesis

The following scenario is proposed for mineral authigenesis in the coal. Formation of authigenic kaolinite and quartz as well as the formation of both cleat sets occurred during early diagenesis (at  $T < 100$  °C). Illite and Na-bearing illite, Fe- and Al-rich chlorite, quartz, and joint set  $J_3$  probably formed during bituminization (100–180 °C).  $\text{NH}_4$ -rich illite, rectorite, pyrophyllite, sudoite, and tosudite all formed during anthracitization ( $T > 200$  °C). The extremely high temperatures associated with anthracitization caused release of large amounts of N from the organic material. Quartz was consumed in areas where pyrophyllite and rectorite formed, and precipitated in areas where sudoite and Fe- and Al-rich chlorite formed. Most of the sulfides appear to have also precipitated during late-stage diagenesis, although the limited evidence does not preclude sulfide precipitation during early diagenesis or after coalification.

Paragenesis in joint set  $J_3$  does not follow the patterns observed in the cleat sets. Dense, anhedral masses of Fe- and Al-rich chlorite and quartz appear to be a result of precipitation from solution, rather than from replacement of an earlier kaolinite/quartz assemblage. Although the basal surfaces of authigenic clays in the cleat sets are oriented perpendicular to the joint surface (Fig. 4), the basal surfaces of Fe- and Al-rich chlorite are oriented parallel to the joint surface, suggesting that the mechanism of Fe- and Al-rich chlorite formation differed fundamentally from that of clay formation in the cleat.

We suggest that the mineralogical differences between high-temperature authigenic clay mineral assemblages in cleat sets  $J_s$  and  $J_{NS}$  reflect permeability differences between the two cleat sets that were controlled by anisotropic Alleghanian stress fields. Differences in permeability would have permitted minerals in each fracture set to equilibrate with two compositionally different fluids. Vitrinite reflectance data from coal seams in Pennsylvania (Levine and Davis, 1989) and systematic joints in strata in the Appalachian foreland basin (Geiser and Engelder, 1983) suggest that a strong lateral compressive stress (directed towards the northwest) was imposed on these strata during coalification and orogenesis, probably owing to the convergence of the North American and African plates in Pennsylvanian time. Such lateral stress would have compressed set  $J_{NS}$ , which has a northeast strike (approximately perpendicular to the inferred convergent stress direction), and probably would have made those joints essentially impermeable. Set  $J_s$ , which has a northwest strike (and, thus, oriented approximately in the plane of the maximum paleostresses prior to deformation), may have dilated temporarily, given sufficiently high pore pressures, and been a permeable conduit for migrating basinal fluids. Fluids in the compressed joints would most likely have been in equilibrium with the surrounding coal matrix because of a low ratio of water to rock, whereas permeable joint sets ( $J_s$ ) would have equilibrated with fluids that were migrating through strata in this region.

The general relationship observed between authigenic clay-mineral assemblages and joint orientations is consistent with the inferred paleohydrology of these coal seams. Al, Si, and N in  $\text{NH}_4$ -rich illite, and Al and Si in pyrophyllite could have been locally derived and, hence, these clays would be expected to have formed in areas with low permeability (shale, coal matrix, and  $J_{NS}$ ), whereas sudoite and tosudite require an external source of Mg and, thus, should only have formed in areas with relatively high permeability ( $J_s$ ). The presence of discrete zones of  $\text{NH}_4$ -rich illite and pyrophyllite in some  $J_s$  cleat is not surprising because migrating fluids would not be expected to have moved uniformly through the systematic cleat and joints. Hydrologic studies (Tsang, 1984; Long and Billaux, 1987) suggest that fluids travel in tortuous paths along joints and that only a fraction of the joints serve as permeable conduits for migrating fluids. Thus,  $J_s$  should have included both high- and low-permeability zones. The minor amounts of  $J_s$ -type minerals

(which commonly occur as veins) in some  $J_{NS}$  joints appear to have resulted from the intersection of systematic and nonsystematic joints.

### CONCLUSIONS

The characterization of minerals in the coal (especially those in the joints) has allowed a more complete interpretation of the origins of the minerals in both the coal and shale. Authigenic kaolinite and quartz formed during early diagenesis ( $T < 100$  °C). Fe- and Al-rich chlorite, illite and Na-bearing illite may have formed at bituminous rank (100–180 °C) from alteration of smectite to illite.  $NH_4$ -rich illite, pyrophyllite, rectorite, tosudite, and sudoite all formed during anthracitization ( $T > 200$  °C) from precursor kaolinite and quartz. Authigenesis in  $J_s$  was influenced by hydrothermal alteration. Much of the N in  $NH_4$ -rich illite was derived from locally abundant organic matter. The majority of N was derived from the coal seams and a significant amount of N was transported into the shale.

Tectonic processes had a significant impact on the diagenetic history of this region. Deformation during the Alleghanian orogeny led to the formation of systematic and nonsystematic joint sets. Lateral compressive stress during the Alleghanian orogeny created permeability differences between opposing cleat sets and thereby led to differences in minerals in the two sets. Mg, Na, and Fe may have been transported through systematic joints in this region, via basal fluid migrations induced periodically by Alleghanian-age uplift. Tectonically induced hydrothermal alteration has influenced diagenesis in this region and may have also significantly influenced coalification by transporting heat, along with solutes, from deeper (and hence hotter) parts of the basin.

### ACKNOWLEDGMENTS

This research was supported by grants from the National Science Foundation (NSF EAR 87-07319), the Petroleum Research Fund of the American Chemical Society (AMER CHEM 18685) and the Geological Society of America (4178-89) and by the Antoinette Lierman Medlin Scholarship Fund. This research would not have been possible without the expert assistance of Jane Eggleston (field guide), Cameron Begg (microprobe analyst) and Don Lowry (low-temperature ashing), and the coal miners of eastern Pennsylvania. We also thank Thomas C. Juster and Sturges W. Bailey for insightful reviews.

### REFERENCES CITED

- Appleman, D.E., and Evans, H.T. (1973) Job 9214: Indexing and least-squares refinement of powder diffraction data. U.S. Geological Survey, Computer Contribution 20, U.S. National Technical Information Service, Document PB2-16188.
- Bailey, S.W. (1980) Structures of layer silicates. In G.W. Brindley and G. Brown, Eds., *Crystal structures of clay minerals and their X-ray identification*, p. 1–125. Mineralogical Society, London.
- Bayliss, P. (1986) Quantitative analysis of sedimentary minerals by X-ray powder diffraction. *Powder Diffraction*, 1, 37–39.
- Boles, J.R., and Franks, S.G. (1979) Clay diagenesis in Wilcox sandstones of southwest Texas: Implications of smectite diagenesis on sandstone cementation. *Journal of Sedimentary Petrology*, 49, 55–70.
- Daniels, E.J. (1989) Origin and distribution of minerals in shale and coal from the Anthracite region, eastern Pennsylvania, 97 p. M.S. thesis, University of Illinois, Urbana, Illinois
- Daniels, E.J., Altaner, S.P., Marshak, S., and Eggleston, J.R. (1990) Hydrothermal alteration in anthracite from eastern Pennsylvania: Implications for mechanisms of anthracite formation. *Geology*, 18, 247–250.
- Deasy, G.F., and Greiss, P.R. (1961) Atlas of Pennsylvania coal and coal mining, part II: Anthracite. Pennsylvania State University Mineral Industries Experiment Station Bulletin, no. 80, 15–25.
- Eberl, D. (1978) The relation of montmorillonite to mixed-layer clay: The effect of interlayer alkali and alkali earth cations. *Geochimica et Cosmochimica Acta*, 42, 1–7.
- Eugster, H.P., and Munoz, J. (1966) Ammonium micas: Possible sources of atmospheric nitrogen. *Science*, 151, 683–686.
- Finkelman, R.B., Yeakel, J., and Harrison, W.J. (1987) Sodium in Upper Cretaceous coal beds of the Wasatch Plateau, Utah: Mode of occurrence, geologic controls, possible source and effects on utilization. *Geological Society of America Abstracts with Programs*, 19, p. 663.
- Fransolet, A.-M., and Bourguignon, P. (1978) Di/trioctahedral chlorite in quartz veins from the Ardennes, Belgium. *Canadian Mineralogist*, 16, 365–373.
- Fransolet, A.-M., and Schreyer, W. (1984) Sudoite, di/trioctahedral chlorite: A stable low-temperature phase in the system  $MgO-Al_2O_3-SiO_2-H_2O$ . *Contributions to Mineralogy and Petrology*, 86, 409–417.
- Geiser, P., and Engelder, T. (1983) The distribution of layer parallel shortening fabrics in the Appalachian foreland of New York and Pennsylvania—Evidence for two non-coaxial phases of the Alleghanian orogeny. In R.D. Hatcher, Jr., H. Williams, and I. Zeitz, Eds., *Contributions to the tectonics and geophysics of mountain chains*. Geological Society of America Memoir 158, 161–175.
- Gluskoter, H.J. (1965) Electronic low temperature ashing of bituminous coal. *Fuel*, 44, 285–291.
- Gradusov, B.P. (1971) Dioctahedral chlorites. *Lithology and Mineral Resources*, 6, 471–478.
- Hatch, J.R., Gluskoter, H.J., and Lindahl, P.C. (1976) Sphalerite in coals from the Illinois Basin. *Economic Geology*, 72, 613–624.
- Hemley, J.J., Montoya, J.W., Marinenko, J.W., and Luce, R.W. (1980) Equilibria in the system  $Al_2O_3-SiO_2-H_2O$  and some general implications for alteration/mineralization processes. *Economic Geology*, 75, 210–228.
- Henderson, G.V. (1971) The origin of pyrophyllite-rectorite in shales of North Central Utah. Utah Geological and Mineralogical Survey, Special Studies no. 34, 46 p.
- Hoffman, J., and Hower, J. (1979) Clay mineral assemblages as low grade metamorphic geothermometers: Application to the thrust faulted disturbed belt of Montana, U.S.A. In P.A. Scholle and P.R. Schluger, Eds., *Aspects of diagenesis: Society of Economic Petrologists and Mineralogists Special Publication no. 26*, p. 55–79.
- Hood, A., Gutjahr, C.C.M., and Heacock, R.L. (1975) Organic metamorphism and the generation of petroleum. *American Association of Petroleum Geologists Bulletin*, 59, 986–988.
- Hosterman, J.W., Wood, G.H., Jr., and Bergin, M.J. (1970) Mineralogy of underclays in the Pennsylvania Anthracite region. U.S. Geological Survey Professional Paper 700-C, C89–C98.
- Hower, J., Eslinger, E.V., Hower, M.E., and Perry, E.A. (1976) Mechanisms of burial metamorphism of argillaceous sediment: I. Mineralogical and chemical evidence. *Geological Society of America Bulletin* 87, 725–737.
- Juster, T.C. (1987) Mineralogic domains in very low grade pelitic rocks. *Geology*, 15, 1010–1013.
- Juster, T.C., Brown, P.E., and Bailey, S.W. (1987)  $NH_4$ -bearing illite in very low-grade metamorphic rocks associated with coal, northeastern Pennsylvania. *American Mineralogist*, 72, 555–565.
- Levine, J.R. (1983) Tectonic history of coal-bearing sediments in eastern Pennsylvania using coal reflectance anisotropy, 288 p. Ph.D. thesis, The Pennsylvania State University, University Park, Pennsylvania.
- (1986) Deep burial of coal-bearing strata, Anthracite region, Pennsylvania: Sedimentation or tectonics? *Geology*, 14, 577–580.
- Levine, J.R., and Davis A. (1989) Reflectance anisotropy of Upper Carboniferous coals in the Appalachian foreland basin, Pennsylvania, U.S.A. *International Journal of Coal Geology*, 13, 341–373.
- Lin, C.-Y., and Bailey, S.W. (1985) Structural data for sudoite. *Clays and Clay Minerals*, 33, 410–414.
- Long, J.C., and Billaux, D.M. (1987) From field data to fracture network

- modeling: An example incorporating spatial structure. *Water Resources Research*, 23, 1201–1216.
- Mackowsky, M.-Th. (1975) Minerals and trace elements occurring in coal. In E. Stach, G.H. Taylor, M.-Th. Mackowsky, D. Chandra, M. Teichmüller, and R. Teichmüller, Eds., *Stach's textbook of coal petrology* (2nd edition), p. 121–131. Gebrüder Borntraeger, Berlin.
- Miser, H.D., and Milton, C. (1964) Quartz, rectorite and cookeite from the Jeffrey quarry near North Little Rock, Pulaski County, Arkansas. *Arkansas Geological Commission, Bulletin 21*, 29 p. Little Rock, Arkansas.
- Morrison, S.J., and Parry, W.T. (1986) Dioctahedral corrensites from Permian red beds, Lisbon Valley, Utah. *Clays and Clay Minerals*, 34, 613–624.
- Nickelsen, R.P. (1979) Sequence of structural stages of the Allegheny orogeny at the Bear Valley strip mine, Shamokin, Pennsylvania. *American Journal of Science*, 279, 225–271.
- Nickelsen, R.P., and Hough, V.N.D. (1967) Jointing in the Appalachian Plateau of Pennsylvania. *Geological Society of America Bulletin*, 78, 609–630.
- Nishiyama, T., and Shimoda, S. (1981) Ca-bearing rectorite from Toho mine, Japan. *Clays and Clay Minerals*, 29, 236–240.
- Paradis, S., Velde, B., and Nicot, E. (1983) Chloritoid-pyrophyllite-rectorite facies rocks from Brittany, France. *Contributions to Mineralogy and Petrology*, 83, 342–347.
- Paxton, S.T. (1983) Relationships between Pennsylvanian-age lithic sandstone and mudrock diagenesis and coal rank in the central Appalachians, 503 p. Ph.D. thesis, Pennsylvania State University, University Park, Pennsylvania.
- Schultz, L.G. (1958) Petrology of underclays. *Geological Society of America Bulletin*, 69, 363–402.
- Shimoda, S. (1969) New data for tosudite. *Clays and Clay Minerals*, 17, 179–184.
- Shirozu, H. (1978) Wall rock alteration of Kuroku deposits. In T. Sudo, and S. Shimoda, Eds., *Clays and clay minerals of Japan: Developments in sedimentology*, 26, 127–145. Elsevier, Tokyo.
- Slatick, E.R. (1980) *Coal data: A reference*, 69 p. U.S. Department of Energy, Washington, D.C.
- Spackman, W., and Moses, R.G. (1961) The nature and occurrence of ash forming minerals in anthracite. In *Proceedings of the anthracite conference*, Nov. 15–16, 1960: Pennsylvania State University Mineral Industries Experiment Station Bulletin, no. 75, p. 1–15.
- Spears, D.A., and Caswell, S.A. (1986) Mineral matter in coals: Cleat forming minerals and their origin in some coals from the English Midlands. *International Journal of Coal Geology*, 6, 107–125.
- Stach, E. (1975) The macerals of coal. In E. Stach, G.H. Taylor, M.-Th. Mackowsky, D. Chandra, M. Teichmüller, and R. Teichmüller, Eds., *Stach's textbook of coal petrology* (2nd edition), p. 54–107. Gebrüder Borntraeger, Berlin.
- Sudo, T., and Shimoda, S., Eds. (1978) *Clays and clay minerals of Japan*, 130 p. Elsevier, Amsterdam.
- Teichmüller, M., and Teichmüller, R. (1975) The geological basis of coal formation. In E. Stach, G.H. Taylor, M.-Th. Mackowsky, D. Chandra, M. Teichmüller, and R. Teichmüller, Eds., *Stach's textbook of coal petrology* (2nd edition), p. 5–54. Gebrüder Borntraeger, Berlin.
- Tillman, J.E., and Barnes, H.L. (1983) Deciphering fracturing and fluid migration histories in northern Appalachian basin. *American Association of Petroleum Geologists Bulletin*, 67, 692–705.
- Tsang, Y. (1984) The effect of tortuosity on fluid flow through a single fracture. *Water Resources Research*, 20, 1209–1215.
- Van der Flier-Keller, E., and Fyfe, W.S. (1988) Mineralogy of Lower Cretaceous coals from the Moose River Basin, Ontario, and Monkman, British Columbia. *Canadian Mineralogist*, 26, 343–353.
- Wood, G.H., Jr., Trexler, J.P., and Kehn, T.M. (1969) Geology of the west-central part of the Southern Anthracite field and adjoining areas, Pennsylvania. U.S. Geological Survey Professional Paper 602, 150 p.

MANUSCRIPT RECEIVED SEPTEMBER 18, 1989

MANUSCRIPT ACCEPTED MAY 28, 1990